Defective interaction between dual oscillators for respiratory rhythm generation in Na^+,K^+-ATPase $\alpha 2$ subunit-deficient mice

Hiroshi Onimaru[1], Keiko Ikeda[2] and Kiyoshi Kawakami[2]

[1]*Department of Physiology, Showa University School of Medicine, 1-5-8 Hatanodai, Shinagawa-ku, Tokyo 142, Japan*
[2]*Division of Biology, Center for Molecular Medicine, Jichi Medical University, Shimotsuke, Tochigi 329-0498, Japan*

The current concept regarding the respiratory centre in mammals is that it is composed of two distinct rhythm-generating neuronal networks in the ventrolateral medulla. These two rhythm generators can be active independently but are normally coupled in newborn and juvenile rats. Detailed characteristics of each generator and the neuronal mechanisms of coupling during development remain to be elucidated. Here, we report a knockout mouse (Na^+,K^+-ATPase $\alpha 2$ subunit gene (*Atp1a2*) knockout) that may be defective in functional coupling between the two respiration-related rhythm generators. We investigated respiration-related neuron activity in an *en bloc* brainstem–spinal cord preparation isolated from embryonic day 18.5 $Atp1a2^{-/-}$ mouse fetuses. In the presence of adrenaline, two different types of rhythm generators were identified. One produced inspiratory burst activity that correlated with C4 inspiratory activity and was thought to be the inspiratory rhythm generator on the basis of its location and sensitivity to a μ-opiate receptor agonist, [D-Ala2, *N*-Me-Phe4, Gly5-ol]-enkephalin (DAMGO). The other was presumed to be the preinspiratory rhythm generator because it was insensitive to DAMGO and correlated with facial nerve activity. Coupling between these rhythm generators did not function in the normal manner in $Atp1a2^{-/-}$ mice, as shown by disruption of the linkage between the preinspiratory burst and the inspiratory burst. Coupling was partially restored by repeated activation of the neurons within the networks, suggesting the involvement of an activity-dependent process in the prenatal development of this coupling.

(Resubmitted 15 May 2007; accepted after revision 9 August 2007; first published online 9 August 2007)
Corresponding author H. Onimaru: Department of Physiology, Showa University School of Medicine, 1-5-8 Hatanodai, Shinagawa-ku, Tokyo 142, Japan. Email: oni@med.showa-u.ac.jp

Breathing is a rhythmic movement in vertebrates. The brainstem contains neurons that participate in the generation of respiratory rhythm activity and other neurons that mediate input by peripheral and central stimuli (Ballanyi *et al.* 1999). There is growing evidence that in mammals, two distinct neuronal networks in the ventrolateral medulla (VLM) are involved in respiratory rhythm generation (Feldman & Del Negro, 2006). One is the pre-Bötzinger complex (pre-BötC) (Smith *et al.* 1991; Rekling & Feldman, 1998), which produces inspiratory (Insp) neuron bursts, and the other is the parafacial respiratory group (pFRG), which produces predominantly preinspiratory (Pre-I) neuron bursts (Onimaru & Homma, 2003; Onimaru *et al.* 2006) or expiratory neuron bursts (Janczewski & Feldman, 2006). These two generators function in close collaboration, although they are also able to work independently, at least under manipulated conditions in newborn and juvenile rats (Mellen *et al.* 2003; Janczewski & Feldman, 2006). How these two rhythm generators contribute to produce spontaneous respiratory rhythm under various experimental conditions remains a matter of debate (Feldman & Janczewski, 2006; Onimaru & Homma, 2006). These rhythm generators can be distinguished by differences in the burst phase, their location in the ventral medulla and their sensitivity to opioids. Although several studies have been performed under conditions in which the interaction was weakened by drugs or was disconnected mechanically (Smith *et al.* 1991; Mellen *et al.* 2003; Janczewski & Feldman, 2006; Onimaru *et al.* 2006), the detailed characteristics of each generator and how each generator is formed and becomes functionally coupled during development remain to be elucidated (Thoby-Brisson *et al.* 2005).

This paper has online supplemental material.

 DOI: 10.1113/jphysiol.2007.136572

Targeted gene disruption of several transcription factors that affect the development of specific groups of brainstem neurons has been reported in mice (Borday *et al.* 2004; Blanchi & Sieweke, 2005). However, there are no reports in which the synaptic interactions between the two generators are disrupted in mice. The Na^+,K^+-ATPase sodium pump is a membrane protein that is essential for maintaining Na^+ and K^+ gradients across the plasma membrane of animal cells. This pump is critical for the support and modulation of electrical activity of excitable cell membranes. The pump consists of α and β subunits. Four α isoforms ($\alpha1$, $\alpha2$, $\alpha3$ and $\alpha4$) have been identified in mammals (for a review, see Lingrel *et al.* 2003). The $\alpha1$ subunit gene is a housekeeping gene that is expressed ubiquitously and is indispensable for early embryonic development. The $\alpha2$ subunit gene is expressed specifically and abundantly in skeletal muscle, heart and brain (Sweadner, 1989). Na^+,K^+-ATPase $\alpha2$ subunit-deficient (*Atp1a2*$^{-/-}$) mouse fetuses die immediately after birth due to severe motor deficits that also abolish respiration (Ikeda *et al.* 2003, 2004). In medullary slice preparations of embryonic day (E)18.5 *Atp1a2*$^{-/-}$ mice, at least one of the rhythm-generating components (probably pre-BötC) is preserved (Moseley *et al.* 2003). It remains unresolved why spontaneous rhythm generation, as monitored by phrenic nerve activity, is not observed in *Atp1a2*$^{-/-}$ fetuses (*in vivo* and *in vitro*) at E18.5. We hypothesized that the failure of respiratory rhythm generation in *Atp1a2*$^{-/-}$ mice is due to dysfunction of the coupling between the pre-BötC and pFRG. To clarify the neuronal organization in the respiratory centre of *Atp1a2*$^{-/-}$ mice, we investigated respiration-related rhythm-generating neuronal groups in the VLM of the brainstem–spinal cord preparation. The results show that functional coupling between the two rhythm generators is incomplete in *Atp1a2*$^{-/-}$ mice and that the coupling can be partially restored by repeated activation of the networks.

Methods

Animals

Mice heterozygous for *Atp1a2* (*Atp1a2*$^{+/-}$) were generated as previously described (Ikeda *et al.* 2004). *Atp1a2*$^{+/-}$ mice were backcrossed 10–12 generations to C57BL/6 mice. Mice lived in a 12 h light/dark cycle. Homozygous (*Atp1a2*$^{-/-}$) embryos were obtained by intercrossing male and female *Atp1a2*$^{+/-}$ mice. Timed pregnancy was defined as E0.5 at noon of the plug date. Fetuses were genotyped by polymerase chain reaction with primers 5′-GGGAGAGACAGACACGGAGGAAGATGAC-3′ and 5′-CCTCCTTCTTCAGCTCATCGAGCTCCTTC-3′ for the wild-type allele and primers 5′-GGGAGAGACAGA-CACGGAGGAAGATGAC-3′ and 5′-GCCTGCTTGCC-GAATATCATGGTGGAAAAT-3′ for the targeted allele.

Recording of nerve activities

Experiments were performed with brainstem–spinal cord preparations from E18.5 fetuses (12 h before full term). In some experiments, 0–1 postnatal day (P0–1) wild-type mice were used as controls. The experimental protocols were approved by the Animal Research Committee of Showa University, which operates in accordance with Law no. 105 for the care and use of laboratory animals of the Japanese Government. E18.5 fetuses were obtained by caesarean section immediately after cervical dislocation of the pregnant mice. Fetal and newborn mice were deeply anaesthetized with ether in a 120 ml glass bottle until nociceptive reflexes induced by tail pinch were abolished. Respiratory movement in wild-type mice halted temporarily at this level of anaesthesia. The cerebrum was quickly removed by transection at the intercollicular level, and the brainstem and spinal cord were isolated according to methods previously described (Suzue, 1984; Onimaru & Homma, 2003). The brainstem was rostrally decerebrated between the VIth cranial nerve roots and the lower border of the trapezoid body. In some experiments, the right half of the pons was retained to monitor facial nerve activity (Onimaru *et al.* 2006). The preparation was superfused at a rate of 3.0 ml min^{-1} with the following artificial cerebrospinal fluid (ACSF) (mM): 124 NaCl, 5.0 KCl, 1.2 KH_2PO_4, 2.4 $CaCl_2$, 1.3 $MgCl_2$, 26 $NaHCO_3$ and 30 glucose, equilibrated with 95% O_2 and 5% CO_2, pH 7.4, at 26–27°C (Suzue, 1984). Inspiratory activity corresponding to phrenic nerve activity was monitored from the fourth cervical ventral root (C4) (Suzue, 1984). In some experiments, nerve activity of the first lumbar ventral root (L1) was also recorded (Janczewski *et al.* 2002). Nerve activities were recorded through a glass suction electrode and high-pass filtered with a 0.3 s time constant. To induce regular respiration-related activity in *Atp1a2*$^{-/-}$ mice, adrenaline (Sigma-Aldrich, St Louis, MO, USA) (Ikeda *et al.* 2004; Viemari & Ramirez, 2006; Fujii *et al.* 2006*a*) or substance P (Peptide Institute, Inc., Osaka, Japan) (Ballanyi *et al.* 1999; Pagliardini *et al.* 2003; Greer *et al.* 2006) was added to the superfusate. The μ-opiate receptor agonist [D-Ala2, *N*-Me-Phe4, Gly5-ol] enkephalin (DAMGO; Sigma-Aldrich) was dissolved in the ACSF and applied by superfusion for 10–15 min.

Whole-cell patch-clamp recordings

Membrane potentials (V_m) and input resistances (R_m) of neurons in the rostral VLM were recorded by a blind whole-cell patch-clamp method (Onimaru & Homma, 1992). The electrodes (inner tip diameter, 1.2–2.0 μm; resistance, 4–8 MΩ) were filled with the following pipette solution (mM): 130 potassium gluconate, 10 ethylene glycol-bis(β-aminoethyl

ether)-*N*,*N*,*N*′,*N*′-tetraacetic acid (EGTA), 10 *N*-2-hydroxy-ethylpiperazine-*N*-ethanesulphonic acid (Hepes), 2 Na_2-ATP, 1 $CaCl_2$ and 1 $MgCl_2$, with pH 7.2–7.3, adjusted with KOH. For histological analysis of the location of recorded cells, the electrode tips were filled with 0.5% Lucifer yellow (lithium salt; Sigma-Aldrich). Membrane potentials were recorded with a single-electrode voltage-clamp amplifier (CEZ-3100; Nihon Kohden Corp., Tokyo, Japan) after compensation for series resistance (20–50 MΩ) and capacitance. After experiments, preparations were fixed for more than 48 h at 4°C in Lillie solution (10% formalin in phosphate buffer, pH 7.0). Transverse 100 μm sections were cut with a laboratory-made vibrating-blade tissue slicer, and Lucifer yellow-labelled neurons were reconstructed with the aid of a camera lucida attached to a fluorescence microscope (BH-2; Olympus Optical Co., Ltd, Tokyo, Japan). Sections were finally stained with neutral red. In some experiments, only extracellular signals were recorded in the conventional cell-attached mode (without giga-seal). Neuronal burst rates and nerve activity (bursts min^{-1}) were calculated from the mean burst activity for 3–5 min. Values are shown as means ± S.D. Statistical significance of differences ($P < 0.05$) was determined by Student's *t* test.

Optical recordings

Each brainstem–spinal cord preparation was placed in ACSF containing a fluorescent voltage-sensitive dye (50 μg ml^{-1} Di-2-ANEPEQ; Molecular Probes, Inc., Eugene, OR, USA) for 40–50 min. After staining, the preparation was placed with the ventral surface up in a 1 ml perfusion chamber mounted on the stage of a fluorescence microscope (BX50WIF-2; Olympus). The preparation was superfused continuously at 2–3 ml min^{-1} with ACSF containing adrenaline or substance P. Neuronal activity in the preparation was detected as changes in fluorescence of the voltage-sensitive dye with the use of an optical recording system (MiCAM01; Brain Vision, Inc., Tsukuba, Japan), as previously described (Onimaru & Homma, 2003). Most recordings were performed with an acquisition time of 20 ms. Fluorescence signals for 6.8 s per trial, including 1.7 s before the trigger signal, were averaged 40–50 times. To detect activity of inspiratory and possibly other respiration-related neurons, C4 inspiratory activity was used as the trigger for optical recordings. To detect activity of non-inspiratory rhythmic neurons, for which activity was not correlated with C4 activity, the extracellular activity from these neurons was used as the trigger. Fluorescence changes were expressed as a ratio (percentage, fractional change) of the fluorescence intensity to that of a reference image. The differential image, processed with a software spatial filter of 2 × 2 pixels, was represented by a pseudocolour display in which red corresponded to a decrease in fluorescence, indicating membrane depolarization. To represent the time course of fluorescence changes in a region of interest, optical signals were inverted.

Electron microscopy

Electron microscopic examination was performed as previously described (Ikeda *et al.* 2003) with the following modification. Small blocks including the VLM (approximately 1 mm^3) dissected from brainstem–spinal cord preparations were fixed in 2% paraformaldehyde and 1% glutaraldehyde in 100 mM cacodylate buffer, pH 7.4, at 4°C for 1 h, and then in 2% glutaraldehyde in the same buffer at 4°C overnight. Synaptic vesicles were counted only when the plasma membrane was clearly defined. We analysed 191 synapses from four *Atp1a2*$^{+/+}$ or *Atp1a2*$^{+/-}$ embryos, 162 synapses from four *Atp1a2*$^{-/-}$ embryos and 171 synapses from three *Atp1a2*$^{-/-}$ embryos subjected to repeated stimulation. Quantitative analysis was performed by a single investigator blinded to mouse genotype. The area measured in each synapse included the presynaptic terminal up to 1 μm from the active zone. The average number of small (~50 nm in diameter) synaptic vesicles per μm^2 was calculated for each preparation. Data are expressed as means ± S.E.M. Differences between groups were examined for statistical significance by one- or two-way ANOVA followed by Fisher's PLSD test in the experiments shown in Fig. 11.

Results

Medullary respiration-related neurons in fetal and newborn wild-type mice

Before describing respiratory neuron activity in *Atp1a2*$^{-/-}$ mice, we describe that of P0–1 and E18.5 wild-type mice as controls. Previous studies have shown that respiratory activity in the brainstem–spinal cord preparation of newborn wild-type mice can be irregular and variable, in contrast to that in rats (Arata *et al.* 1997; Ptak & Hilaire, 1999). This irregular activity can be changed to a regular pattern in the presence of a low concentration of adrenaline (Arata *et al.* 1997) (online supplemental material, Supplemental Fig. 1). Here, we describe several types of respiration-related neurons, Insp and Pre-I neurons, in the VLM of medulla-spinal cord preparations of wild-type mice, in the presence of 0.1–0.2 μM adrenaline. The rate and duration of C4 inspiratory activity were 9.5 ± 5.2 bursts min^{-1} and 837 ± 416 ms in newborn mice and 15.3 ± 7.1 bursts min^{-1} and 234 ± 118 ms in E18.5 mice, respectively. The burst rate was higher in E18.5 mice than in newborn mice ($P < 0.05$), and the duration was

shorter in E18.5 mice than in newborn mice ($P < 0.001$). In newborn mice, Insp neurons (V_m, -50.2 ± 4.0 mV; R_m, 466 ± 205 MΩ; $n = 9$) were classified into three subtypes, as described in newborn rat preparations, and postsynaptic potentials during the postinspiratory phase were less typical in mice than in rats (Fig. 1). Type I neurons ($n = 5$) showed excitatory postsynaptic potentials (EPSPs) prior to the onset of inspiratory nerve discharge (Fig. 1*A*). In type II neurons ($n = 2$), EPSPs only occurred during the inspiratory phase (Fig. 1*B*), whereas type III neurons ($n = 2$) were hyperpolarized by synchronized inhibitory postsynaptic potentials (IPSPs) during the preinspiratory phase (Fig. 1*C*). Pre-I neurons (V_m, -50.0 ± 5.5 mV; R_m, 502 ± 185 MΩ; $n = 7$) in newborn mice were classified into two subtypes, type I showing action potential discharges predominantly during the preinspiratory phase ($n = 5$; Fig. 1*D*) and type II showing discharges during the pre- and postinspiratory phases ($n = 2$; Fig. 1*E*).

In E18.5 mice, we recorded Insp neurons (V_m, -50.3 ± 7.2 mV; R_m, 413 ± 137 MΩ; $n = 7$) corresponding to type I ($n = 4$, Fig. 2*A*), type II ($n = 2$) and type III ($n = 1$; Fig. 2*B*) Insp neurons of newborns, and Pre-I neurons (V_m, -50.7 ± 4.3 mV; R_m, 455 ± 212 MΩ; $n = 6$) corresponding to type I ($n = 5$, Fig. 2*C*) and type II ($n = 1$) Pre-I neurons of newborns. Some of these respiratory neurons were stained by Lucifer yellow, and their locations were plotted in Fig. 6. Thus, the respiratory neuron network in fetal and newborn mouse medulla is thought to be similar to that in newborn rats; excitatory synaptic connections from Pre-I to Insp neurons and inhibitory synaptic connections from Pre-I to Insp neurons and from Insp to Pre-I neurons, whereas the majority of Pre-I neurons are type I in mouse and type II in rat (Ballanyi *et al.* 1999).

Inspiratory neurons in knockout mice

Spontaneous C4 inspiratory activity is not produced in the brainstem–spinal cord preparation of *Atp1a2*$^{-/-}$ mice; however, application of a neurostimulant (adrenaline) induces regular C4 activity (Ikeda *et al.* 2004). In preliminary experiments in this study, we tested several neurostimulants (adrenaline, substance P, thyrotropin-releasing hormone (TRH) and high K^+ in the bath) for the ability to induce C4 activity. Adrenaline and substance P induced regular and stable C4 inspiratory activity, whereas TRH and high K^+ in the bath induced strong tonic C4 discharges, accompanied by less stable inspiratory activity. The opiate antagonist naloxone, which has been reported to activate respiratory rhythm in newborn mice (Jacquin *et al.* 1996), was not effective in facilitating respiratory rhythm in *Atp1a2*$^{-/-}$ mice. Therefore, we used adrenaline and substance P as neurostimulants in the present experiments. As shown below, repeated application of these substances resulted in time-dependent changes in respiratory network activity.

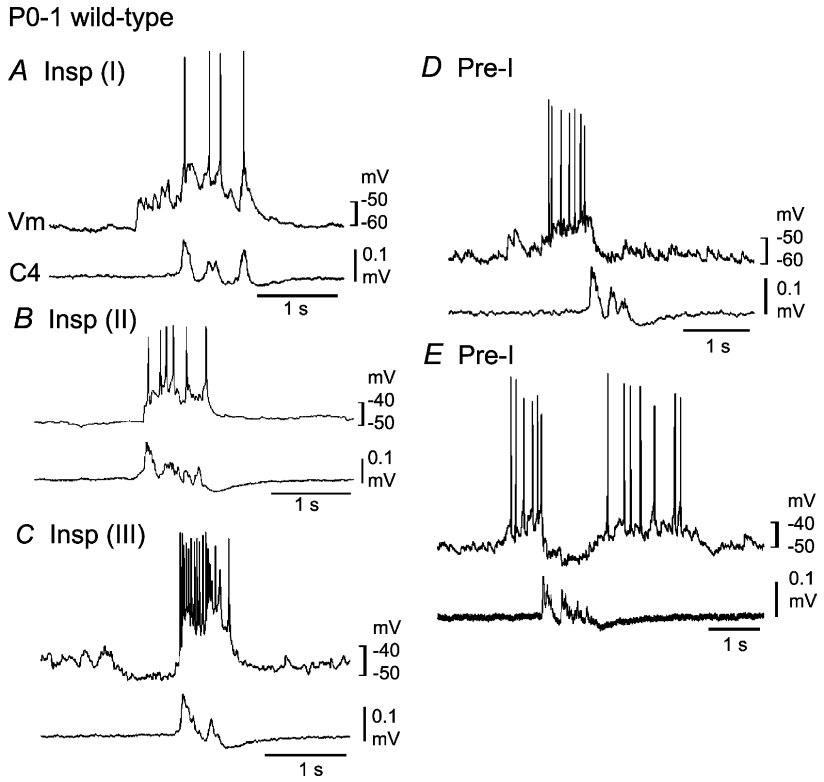

Figure 1. Respiratory neurons in the ventrolateral medulla of neonatal wild-type mice
Neurons were recorded in the ventrolateral medulla of the brainstem–spinal cord preparation (without pons) from postnatal day 0–1 wild-type mice in the presence of 0.1–0.2 μM adrenaline (see supplemental Fig. 1 for activity in the absence of adrenaline). *A*, a type I inspiratory (Insp) neuron receiving excitatory postsynaptic potentials (EPSPs) prior to onset of inspiratory nerve discharge. *B*, a type II Insp neuron in which EPSPs occur only during the inspiratory phase. *C*, a type III Insp neuron hyperpolarized by synchronized inhibitory postsynaptic potentials (IPSPs) during the preinspiratory phase. *D*, a type I preinspiratory (Pre-I) neuron showing action potential discharges predominantly during the preinspiratory phase. *E*, a type II Pre-I showing action potential discharges during pre- and postinspiratory phases. V_m, membrane potential trajectory; C4, C4 inspiratory activity.

This effect appeared to be stronger with substance P than with adrenaline, and therefore we used predominantly adrenaline for membrane potential recordings of rhythmically active neurons to examine the basic neuron network in *Atp1a2*$^{-/-}$ mice before measuring time-dependent changes of network properties induced by neurostimulants. First, we used 3–5 μM adrenaline to induce C4 inspiratory bursts, as reported previously (Ikeda *et al.* 2004), and recorded, extracellularly or intracellularly, respiration-related neuronal activity in the VLM (see Fig. 6 for locations). The burst rate and duration of C4 activity were $1.4 \pm 0.9\,\text{min}^{-1}$ and 970 ± 163 ms ($n = 12$) in response to 3 μM adrenaline and $1.9 \pm 0.7\,\text{min}^{-1}$ and 921 ± 340 ms ($n = 21$) in response to 5 μM adrenaline, respectively. The inspiratory rhythm was significantly ($P < 0.001$) slower than that in wild-type mice. The burst duration was comparable to that of wild-type P0–1 mice but was significantly ($P < 0.001$) longer than that of wild-type E18.5 mice. Thus, this adrenaline-induced inspiratory activity may correspond to sigh burst (see below).

In the presence of adrenaline, rhythmically active (i.e. Insp) neurons, the activity of which was in phase with C4 activity, were identified in the VLM (rate, $1.3 \pm 0.8\,\text{min}^{-1}$; $n = 15$). Burst discharge was not detected in the absence of adrenaline. Insp neurons (V_m, -49.0 ± 3.8 mV; R_m, 535 ± 204 MΩ) were categorized into three subtypes: a type receiving clustered EPSPs ($n = 8$; Fig. 3*A*), a type receiving neither clustered EPSPs nor clustered IPSPs, ($n = 4$; Fig. 3*B*) and a type receiving clustered IPSPs ($n = 3$; data not shown). These subtypes presumably correspond to type I, type II and type III Insp neurons of wild-type mice. The rate of clustered EPSPs was $5.1 \pm 1.2\,\text{min}^{-1}$, and that of clustered IPSPs was $4.8 \pm 0.8\,\text{min}^{-1}$. These results indicated that many Insp neurons receive synaptic inputs from other neurons with burst rates higher than that of the inspiratory activity in the presence of adrenaline. To evaluate the relation between inspiratory bursts and clustered EPSPs, we averaged the membrane potential and used the onset of C4 activity as a trigger signal in three typical preparations. Results suggested that inspiratory burst activity, as monitored by C4 activity, is not associated with clustered EPSPs (Fig. 3*A*′).

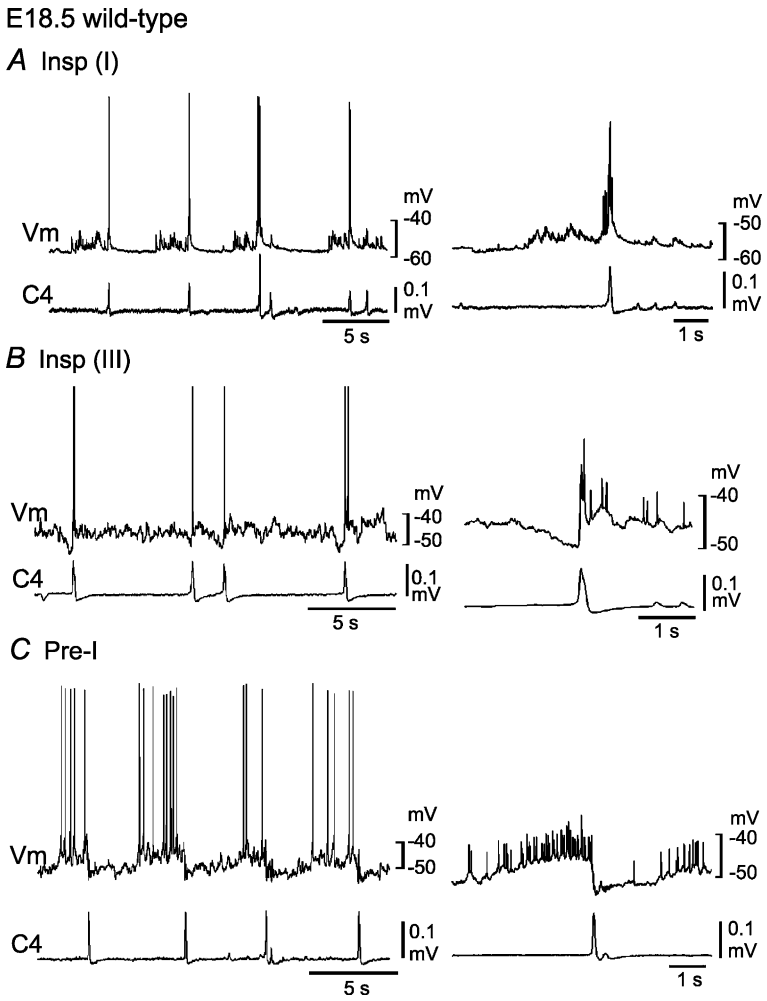

Figure 2. Respiratory neurons in the ventrolateral medulla of embryonic day 18.5 wild-type mice
Neurons were recorded in the ventrolateral medulla of the brainstem–spinal cord preparation (without pons) from embryonic day 18.5 wild-type mice in the presence of 0.1–0.2 μM adrenaline. *A*, a type I inspiratory (Insp) neuron receiving excitatory postsynaptic potentials (EPSPs) during the preinspiratory phase. *B*, a type III Insp neuron hyperpolarized by synchronized inhibitory postsynaptic potentials (IPSPs) during the preinspiratory phase. *C*, a type I preinspiratory (Pre-I) neuron showing action potential discharges predominantly during the preinspiratory phase. Right panels, membrane potential averaged 6 (in *A*) and 10 (in *B* and *C*) times with the use of C4 activity as a trigger. V_m, membrane potential trajectory; C4, C4 inspiratory activity.

Non-inspiratory rhythmic neurons in knockout mice

We next sought the putative source neurons producing clustered EPSPs or IPSPs in the Insp neurons with the idea that these neurons could be putative Pre-I neurons. We recorded non-inspiratory rhythmically active neurons in the VLM (see Fig. 6 for locations) in the presence of 3–5 μM adrenaline. The mean burst rate (5.7 ± 1.6; $n = 17$) was significantly higher than that of C4 inspiratory activity ($P < 0.001$) and was similar to that of the clustered EPSPs of Insp neurons (see above). Of the intracellularly recorded neurons (V_m, -46.1 ± 3.9 mV; 553 ± 182 MΩ; $n = 10$), six received EPSPs during inspiratory activity (Fig. 4*A*), and four received IPSPs during inspiratory activity (Fig. 4*B*). We examined the effects of a lower concentration of adrenaline on the burst activity. The burst rate of C4 inspiratory activity in response to 0.5 μM adrenaline (0.5 ± 0.1 min^{-1}; $n = 10$) was significantly lower than that in the presence of 5 μM adrenaline, whereas the burst rate of non-inspiratory rhythmic neurons was not significantly changed in response to 0.5 μM adrenaline (6.2 ± 1.2 min^{-1}; $n = 10$, Fig. 5). These results indicate a difference in sensitivity to adrenaline between non-inspiratory rhythmic neurons and Insp neurons. We speculated that non-inspiratory rhythmic neurons could be the source for clustered EPSPs or IPSPs in the Insp neurons, producing a latent network respiratory rhythm. The timing of the burst generation did not correlate with inspiratory activity (Fig. 4). Our findings indicated that the non-inspiratory rhythmic neurons (i.e. putative Pre-I neurons, see below) in the VLM of *Atp1a2*$^{-/-}$ mice form characteristically distinct neuron groups from Insp neurons.

Characteristics of respiration-related neurons in knockout mice

The above observations suggested the existence of at least two neuronal populations that produce rhythmic activity in the VLM of *Atp1a2*$^{-/-}$ mice. In the rat, two distinct rhythm generators (the pre-BötC and pFRG) in the medulla show differential sensitivity to DAMGO (an opiate agonist), different facial nerve output patterns and

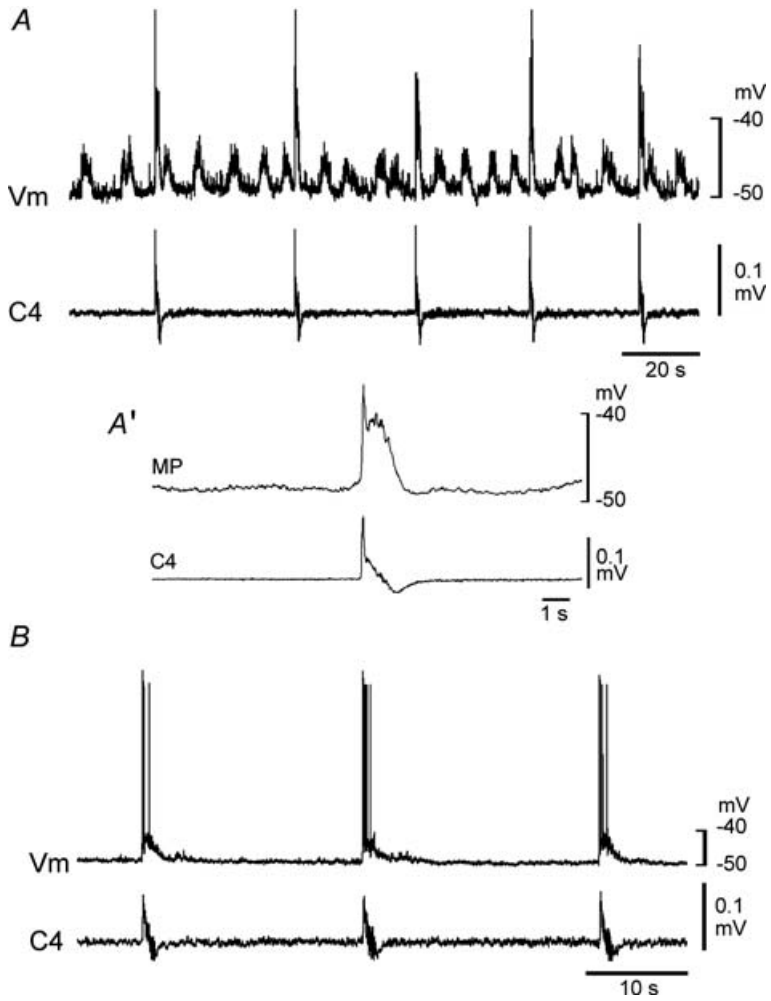

Figure 3. Inspiratory neurons in the ventrolateral medulla of *Atp1a2*$^{-/-}$ mice
Burst activity was induced by application of 5 μM adrenaline. *A*, an inspiratory neuron receiving clustered excitatory postsynaptic potentials (EPSPs). *A'*, membrane potential averaged 24 times with the use of C4 activity as a trigger. *B*, an inspiratory neuron receiving neither clustered EPSPs nor clustered inhibitory postsynaptic potentials (IPSPs). Note the absence of clear EPSPs associated with inspiratory bursts. The threshold for action potential generation was approximately −40 and −35 mV in the neuron in *A* and the neuron in *B*, respectively. V_m, membrane potential trajectory; C4, C4 inspiratory activity.

a distinct rostrocaudal distribution of neurons (Takeda *et al.* 2001; Mellen *et al.* 2003; Onimaru & Homma, 2003, 2006). Therefore, we examined the effect of 1 μM DAMGO in *Atp1a2*$^{-/-}$ mice. The non-inspiratory rhythmic neuron shown in Fig. 4*B* showed IPSPs corresponding to C4 inspiratory activity in response to 5 μM adrenaline. Bath application of DAMGO resulted in the disappearance of these IPSPs and of C4 inspiratory activity but did not alter the rhythmic non-inspiratory activity (Fig. 4*C*). Similar results were obtained for all neurons tested ($n = 5$ in five preparations, four neurons receiving IPSPs and one neuron receiving EPSPs during inspiratory activity). These results indicate that non-inspiratory rhythmic activity in *Atp1a2*$^{-/-}$ mice is less sensitive to DAMGO than is inspiratory activity.

We next examined whether non-inspiratory burst activity correlated with facial nerve activity because motor output can be used to monitor Pre-I neuron activity (Onimaru & Homma, 2006). In response to 0.5 μM adrenaline, the facial nerve exhibited rhythmic activity synchronized with non-inspiratory rhythmic activity, as shown in Fig. 5*B* and *B*′. The burst rate of the rhythmic facial nerve activity was 6.7 ± 1.1 min^{-1} ($n = 5$). These results indicate that facial nerve activity is in phase with the rhythmic activity of non-inspiratory neurons.

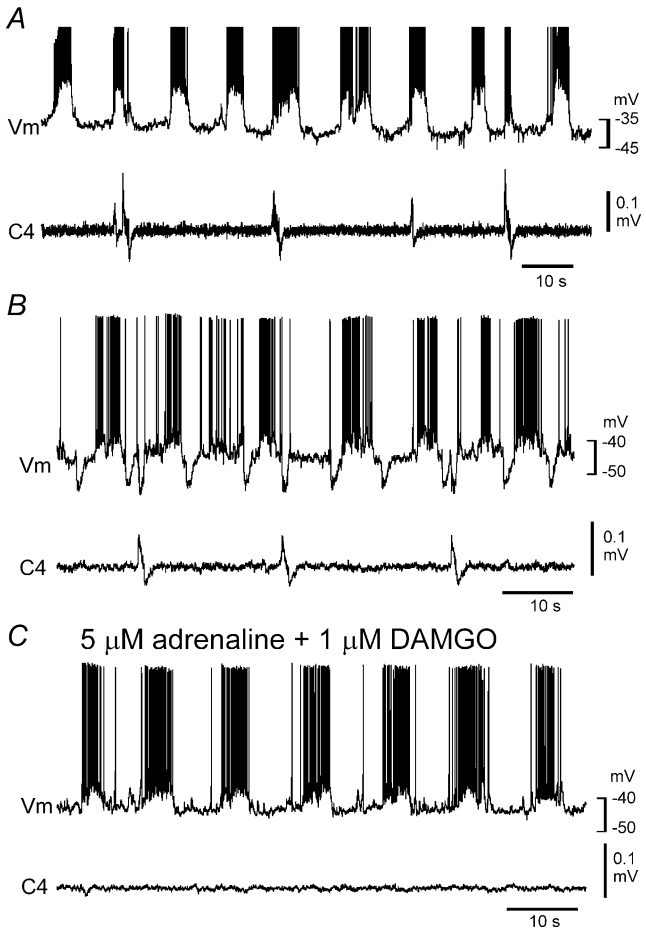

Figure 4. Non-inspiratory rhythmic neurons in the ventrolateral medulla of *Atp1a2*$^{-/-}$ mice
Recording was performed in the presence of 5 μM adrenaline. *A*, a non-inspiratory rhythmic neuron that was also active during the inspiratory phase. *B*, a non-inspiratory rhythmic neuron receiving inhibitory postsynaptic potentials (IPSPs). *C*, application of 1 μM DAMGO (a μ-opiate agonist) inhibited C4 inspiratory activity and all clustered IPSPs in this neuron, whereas the burst activity of the non-inspiratory rhythmic neuron was preserved. V_m, membrane potential trajectory; C4, C4 inspiratory activity.

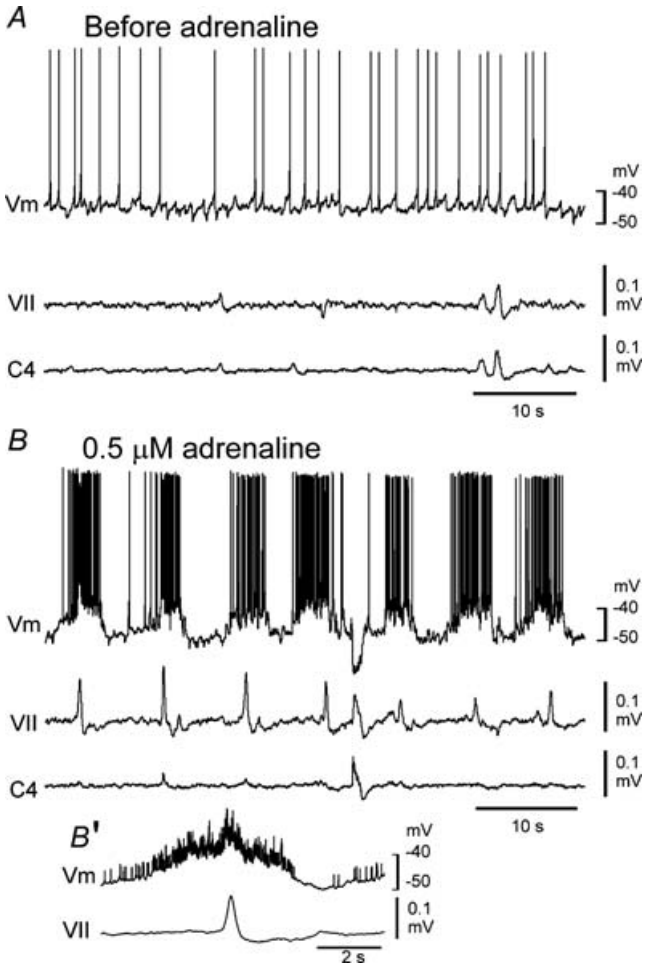

Figure 5. Burst activity of a non-inspiratory neuron and facial nerve activity induced by a low concentration of adrenaline in the ventrolateral medulla of *Atp1a2*$^{-/-}$ mice
A, membrane potential trajectory in control solution. Note the lack of burst activity. *B*, after a 5 min application of 0.5 μM adrenaline, burst activity of the neuron and corresponding facial nerve activity are induced. *B*′, membrane potential averaged 12 cycles with the use of facial nerve activity as a trigger. This neuron received inhibitory postsynaptic potentials during the inspiratory phase. V_m, membrane potential trajectory; VII, facial nerve activity; C4, C4 inspiratory activity.

Distribution of respiration-related burst neurons in knockout mice

Inspiratory and non-inspiratory burst neurons were stained with Lucifer yellow after membrane potential recording, and the locations of these neurons are shown in Fig. 6. The neurons were located ventral to the nucleus ambiguus and caudal to the facial nucleus. To obtain a more comprehensive distribution of these neurons, we performed optical recordings of neuronal activity in the VLM. To visualize inspiratory neuron activity, we used C4 activity as a trigger in the presence of 5 μM adrenaline (Ikeda *et al.* 2004). Activity during the inspiratory burst was observed in the VLM at the level of (or slightly rostral to) the most rostral roots of the XIIth cranial nerve (Fig. 7*A*, Supplemental Movie 1). To visualize non-inspiratory rhythmic neuron activity, we recorded the extracellular spike activity of the burst neurons and performed image averaging with the use of the initiation points of the spike train as a trigger for optical recordings in the presence of 5 μM adrenaline. Activity was located predominantly in the rostral VLM overlapping the area containing pFRG/Pre-I neurons (Fig. 7*B*, Supplemental Movie 2) and was similar to activity during the preinspiratory phase in wild-type mice (Onimaru & Homma, 2003; Onimaru *et al.* 2004). The most active region was at the level of the facial nucleus, and thus the optical signal may also reflect activity of facial motor neurons (Onimaru *et al.* 2004).

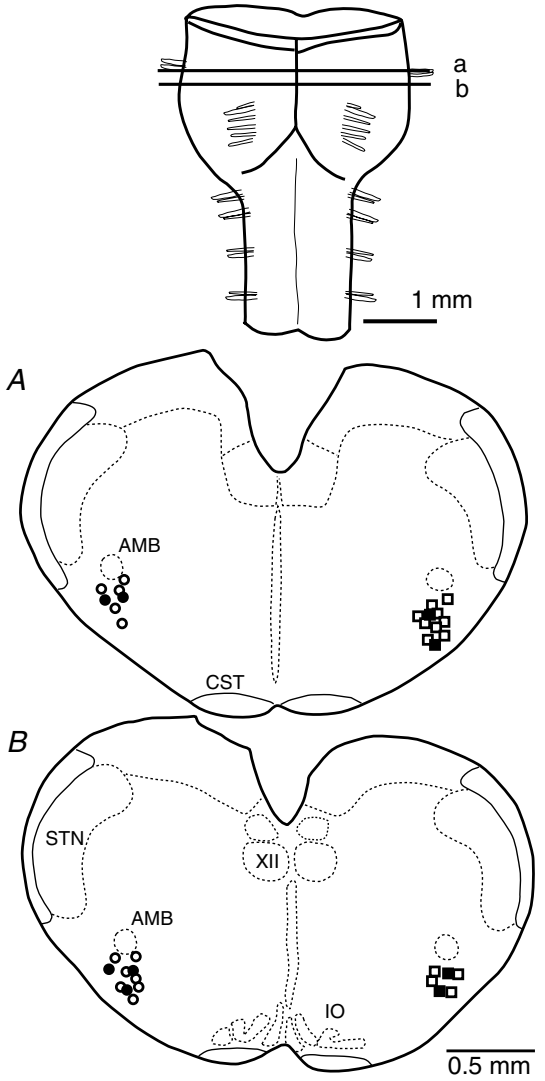

Figure 6. Location of recorded neurons in the ventrolateral medulla of embryonic day 18.5 wild-type and *Atp1a2*$^{-/-}$ mice
Neurons (in embryonic day18.5 preparations) stained with Lucifer yellow were recorded within ± 100 μm of the lines (a and b) indicating the rostral and caudal positions of cross-section and are plotted in two sections (A and B) below. ○ and ● circles, inspiratory neurons in *Atp1a2*$^{-/-}$ mice and wild-type mice, respectively; □ and ■ squares, non-inspiratory rhythmic neurons in *Atp1a2*$^{-/-}$ mice and preinspiratory neurons in wild-type mice, respectively. AMB, nucleus ambiguus; CST, corticospinal tract; IO, inferior olivary nucleus; STN, spinal trigeminal nucleus; XII, hypoglossal nucleus.

Changes in network properties

Episodic application of neurostimulant agonists to motoneurons elicits persistent changes in motoneuronal output by potentiating postsynaptic function (Bocchiaro & Feldman, 2004). To determine whether network activation improved respiration-related nerve activity in *Atp1a2*$^{-/-}$ mice, we examined the effects of episodic neuronal stimulation on C4, facial and L1 nerve activity (Janczewski *et al.* 2002; Onimaru *et al.* 2006). Repeated (3–5) applications of adrenaline or substance P resulted in an increased C4 burst rate (Figs 8 and 9). The initial application of 0.5 μM adrenaline induced rhythmic facial nerve activity ($8.1 \pm 1.0\,\text{min}^{-1}$; $n = 3$) and a low C4 burst rate ($0.42 \pm 0.07\,\text{min}^{-1}$; Fig. 8*A*). The C4 burst rate increased gradually in response to repeated application of adrenaline for 10 min with 10 min intervals (see also Fig. 9*C*). Facial nerve and C4 activities during the fifth application of adrenaline are shown in Fig. 8*B*. The facilitated C4 activity ($5.8 \pm 0.76\,\text{min}^{-1}$) appeared in association with the facial nerve activity ($8.1 \pm 0.85\,\text{min}^{-1}$; Fig. 8*B* and *Ca*), and the facial nerve activity preceded C4 activity for 1320 ± 305 ms (Fig. 8*Cb*). Consistent results were obtained in seven preparations. In three preparations, L1 activity was also monitored. After repeated application of adrenaline, L1 activity appeared during the preinspiratory phase, as did facial nerve activity (Fig. 8*D*). Similar results were obtained in response to repeated application of 100 nM substance P in 11 preparations (Fig. 9). The increase of the C4 burst rate in response to repeated application of substance P is summarized in Fig. 9*C*. The facilitated C4 burst rate ($9.1 \pm 3.8\,\text{min}^{-1}$; duration, 235 ± 96.0 ms; $n = 18$) was typically interrupted by larger amplitude inspiratory activity with a slower

burst rate ($0.6 \pm 0.2\,\text{min}^{-1}$; duration, 931 ± 64.2 ms; Figs 8*B* and 9*A*).

It is necessary to compare the activity induced by repetitive stimulation in *Atp1a2*$^{-/-}$ mice with that of wild-type (or heterozygous) mice. We recorded facial nerve, C4 and L1 activities in preparations of E18.5 wild-type and heterozygous mice. Many preparations (approximately 80%) initially showed irregular respiratory activity (Supplemental Fig. 2). This irregular activity became regular after the administration of 0.1 μM adrenaline (Fig. 10). Facial and L1 activities in the presence of 0.1 μM adrenaline preceded C4 inspiratory bursts for 1960 ± 496 ms ($n = 3$; Fig. 10*A*′ and *B*), similar to rat preparations (Janczewski *et al.* 2002; Onimaru *et al.* 2006), whereas postinspiratory activity was not detectable. Over a longer time period, the faster C4 rhythm (rate, $10.5 \pm 1.5\,\text{min}^{-1}$; duration, 264 ± 17.2 ms; $n = 11$) was interrupted by slower, larger amplitude activity (rate, $0.6 \pm 0.1\,\text{min}^{-1}$; duration, 781 ± 155 ms; $n = 11$; Fig. 10*A*). Consequently, nerve activity patterns in *Atp1a2*$^{-/-}$ mice after repetitive stimulation (Figs 8 and 9) resembled those of wild-type or heterozygous mice in the presence of 0.1 μM adrenaline.

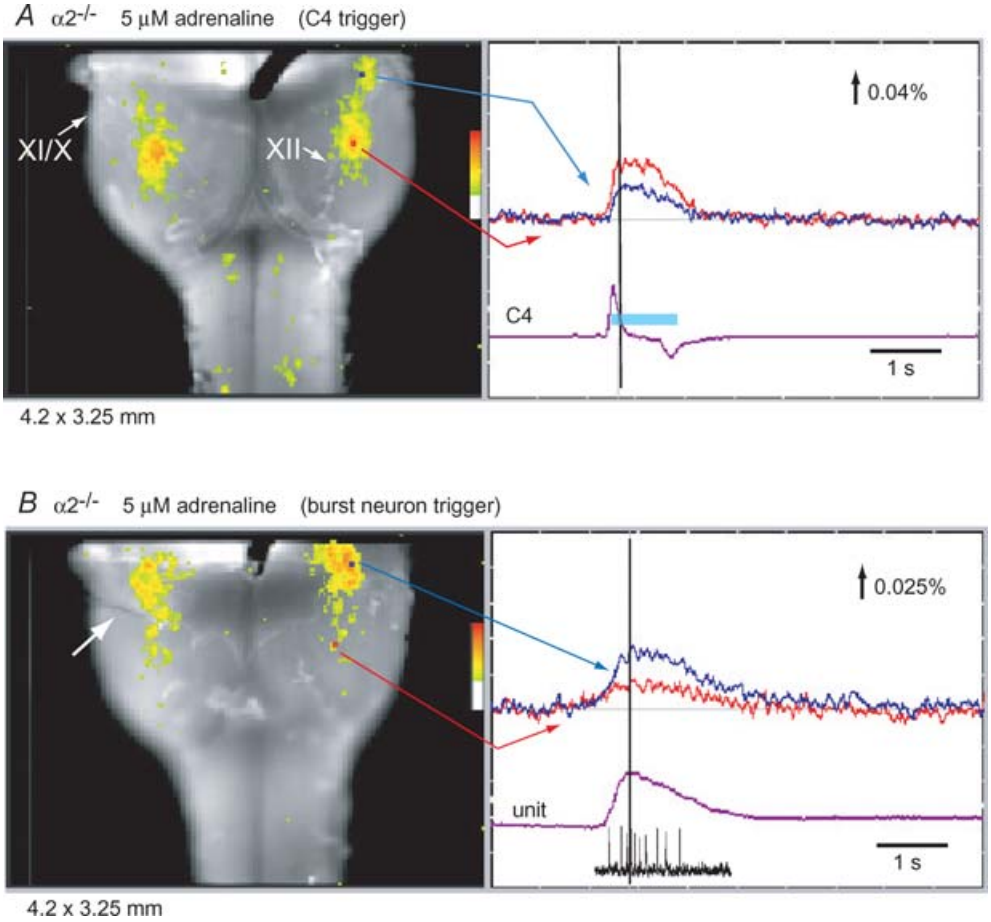

Figure 7. Optical recordings of respiration-related neuron activity in the ventral medulla of Atp1a2$^{-/-}$ mice

A, inspiratory neuron activity. Left panel, optical image of inspiratory neuron activity near the C4 peak (at black vertical line in the right trace) superimposed on the ventral surface of the medulla. IX/X and XII are the IX/Xth and the XIIth cranial nerve roots, respectively. Right panel, tracing of fluorescence changes at two different locations on the medulla: blue, at the level of the facial nucleus; red, at the level of the rostral roots of the XIIth cranial nerve. Fluorescence decrease (i.e. depolarization) is upward. The purple trace (C4) represents C4 inspiratory activity. The light-blue bar on the C4 trace denotes the inspiratory phase. Results are the average of 40 respiratory cycles triggered by C4 inspiratory activity. *B*, non-inspiratory burst neuron activity. Left panel, optical image of burst neuron activity near the peak spike discharge (at black vertical line in the right trace) superimposed on the ventral surface of the medulla. Right panel, tracing of fluorescence changes at two different locations on the medulla: blue, at the level of the facial nucleus; red, at the level of the rostral roots of the XIIth cranial nerve. The purple trace (unit) represents integrated spike discharge with a typical discharge pattern below the trace. Results are the average of 30 bursts triggered by an initial spike of unit discharge recorded extracellularly by a glass electrode (white arrow in the left panel).

Despite the functional defects in respiratory rhythm generation in *Atp1a2*$^{-/-}$ mice, no clear abnormality in brainstem morphology was found at the light microscopic level (K. Ikeda, unpublished observations). To identify possible anomalies in ultramicroscopic structures, we examined synaptic morphology in the VLM of knockout mice before and after repetitive stimulation with substance P and compared the results with those of wild-type and heterozygous mice. This VLM region, at a level slightly rostral to the most rostral roots of the XIIth nerve, corresponded to the region that indicated robust inspiratory activity (Fig. 7*A*). The general appearance and number of presynaptic terminals were similar between *Atp1a2*$^{-/-}$ and *Atp1a2*$^{+/+}$ or *Atp1a2*$^{+/-}$ mice. However, the number of active synaptic vesicles near the active zones in *Atp1a2*$^{-/-}$ mice was significantly decreased compared to that of *Atp1a2*$^{+/+}$ or *Atp1a2*$^{+/-}$ mice (Fig. 11). Active vesicles were defined as those located up to 1 μm from the active zone. The mean numbers were 23.8 ± 1.0 ($n = 4$) in *Atp1a2*$^{-/-}$ mice, and 49.6 ± 11.8 ($n = 4$) in *Atp1a2*$^{+/+}$ or *Atp1a2*$^{+/-}$ mice (ANOVA, $P < 0.04$). After repeated stimulation with 100 nM substance P, an increase in the number of vesicles was observed in *Atp1a2*$^{-/-}$ mice (35.0 ± 3.9; $n = 3$) (Fig. 11*B*).

Discussion

Previous studies, mainly in rats, have determined the existence of two rhythm generator systems in the medullary respiratory centre: the pre-BötC-inspiratory rhythm generator corresponding to C4 inspiratory activity (Smith *et al.* 1991; Rekling & Feldman, 1998) and the pFRG-Pre-I rhythm generator reflected in facial nerve activity (Onimaru & Homma, 2003, 2006). The latter appears to be equivalent to the expiratory rhythm generator that was proposed in *in vivo* experiments in rats by Janczewski & Feldman (2006), whereas Pre-I neurons in the newborn rat preparation are not identical to expiratory neurons (Arata *et al.* 1998; see Onimaru *et al.* 2006 for detailed discussion). These two generators

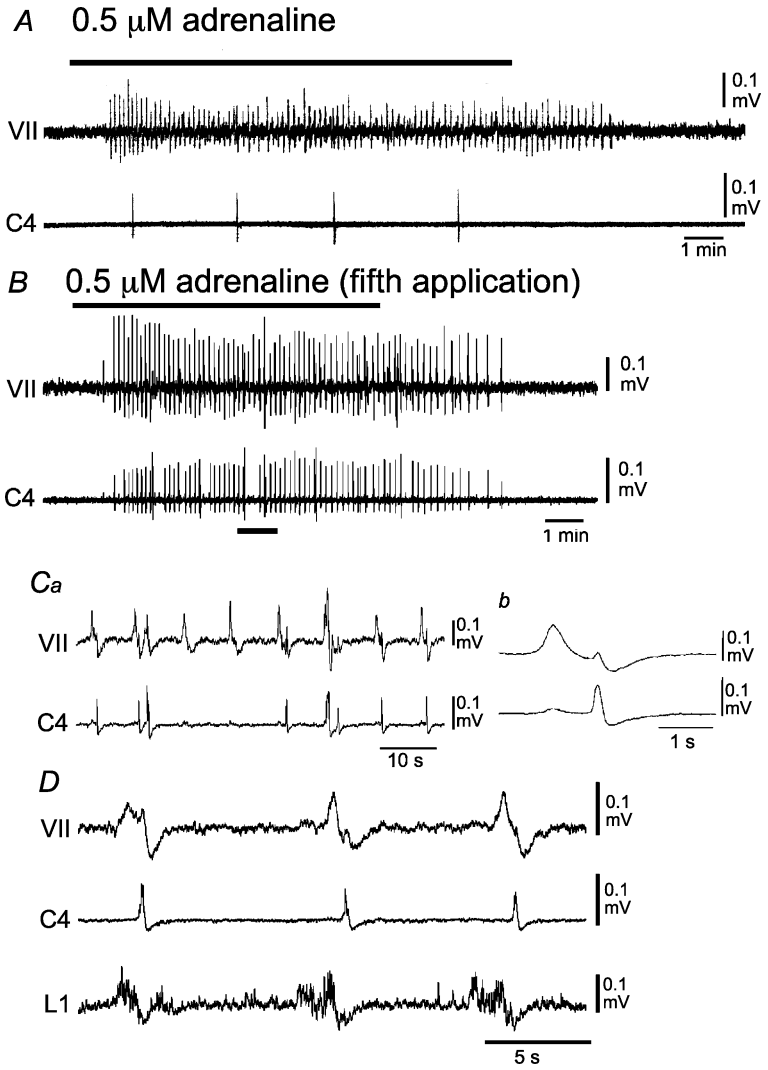

Figure 8. Effects of repeated application of adrenaline on facial, C4 and L1 activities in *Atp1a2*$^{-/-}$ mice
A, the initial application of 0.5 μM adrenaline after starting superfusion induced a high-frequency rhythmic burst in the facial nerve but not in C4. *B*, high-frequency bursts in both nerves are induced during the fifth 10 min application of adrenaline with 10 min intervals between applications. *Ca*, faster sweep representation of facial and C4 nerve activities at the black bar in *B*. *Cb*, averaged facial nerve activity triggered by C4 (10 cycles). Note that the facial nerve burst precedes the C4 inspiratory burst. *D*, facial, C4 and L1 nerve activities during the third application of 0.5 μM adrenaline. Note that L1 activity appeared during the preinspiratory phase. VII, facial nerve activity; C4, C4 inspiratory activity; L1, first lumbar ventral root activity.

interact in the intact brainstem to form a coupled oscillator (Mellen *et al.* 2003; Janczewski & Feldman, 2006). Electrophysiological and optical recording studies have shown sequential activation of Pre-I and Insp neurons in the mouse brainstem–spinal cord preparation (Onimaru *et al.* 2004), suggesting that the organization of respiratory neuron networks in the mouse preparation is similar to that of the newborn rat preparation (Arata *et al.* 1997). In the present study, we further confirmed this similarity in wild-type mouse preparations. We then showed the existence of at least two functionally independent rhythm generators in *Atp1a2*$^{-/-}$ mice, which may comprise a coupled oscillator system in wild-type mice. This is the first report of mice lacking functional interaction between the two rhythm generators.

Characteristics of the two types of burst neurons

Atp1a2$^{-/-}$ mice do not produce regular respiratory rhythm *in utero* or after birth (Ikeda *et al.* 2003, 2004; Moseley *et al.* 2003). In the presence of adrenaline, we identified at least two types of burst neurons with different characteristics in the VLM. One type showed activity synchronized with C4 inspiratory activity and was thus thought to comprise inspiratory neurons. Activity of these neurons was inhibited by DAMGO, and the main region of activity, as determined by optical recording, was localized at the level of (or slightly rostral to) the most rostral roots of the XIIth nerve, partially overlapping the area of the pre-BötC. Thus, we concluded that this group includes neurons corresponding to (or closely correlating with) the pre-BötC-Insp rhythm generator. The other type showed a

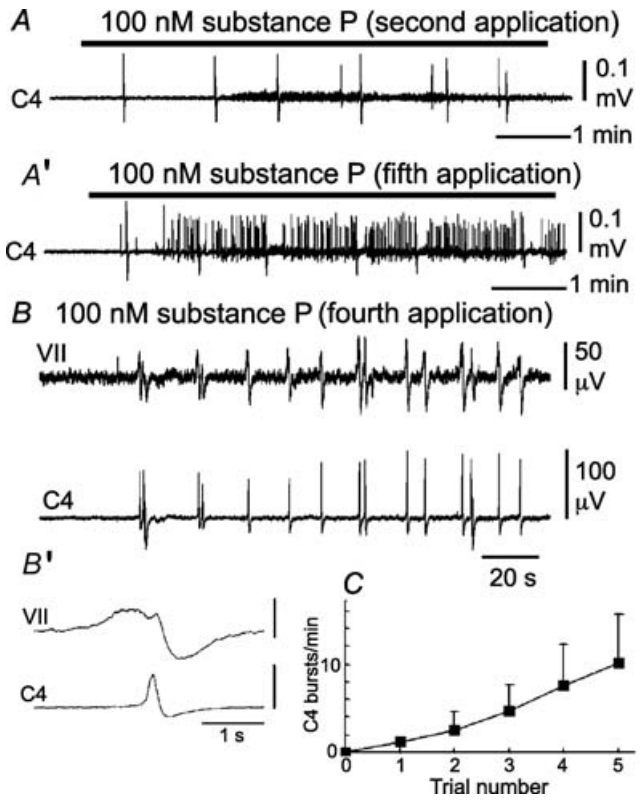

Figure 9. Effects of substance P on facial and C4 nerve activities in *Atp1a2*$^{-/-}$ mice
A, C4 nerve activity during the second application of 100 nM substance P. *A*′, C4 nerve activity during the fifth application of substance P. *B*, facial and C4 nerve activities during the fourth application of 100 nM substance P in a different preparation. Substance P induced high-frequency bursts in both nerves. *B*′, averaged facial nerve activity triggered by C4 (10 cycles). Note that the facial nerve burst precedes the C4 inspiratory burst. *C*, increase of C4 burst rate in response to repeated application of 100 nM substance P for 10 min with 10 min intervals. Values are averaged from five preparations. VII, facial nerve activity; C4, C4 inspiratory activity.

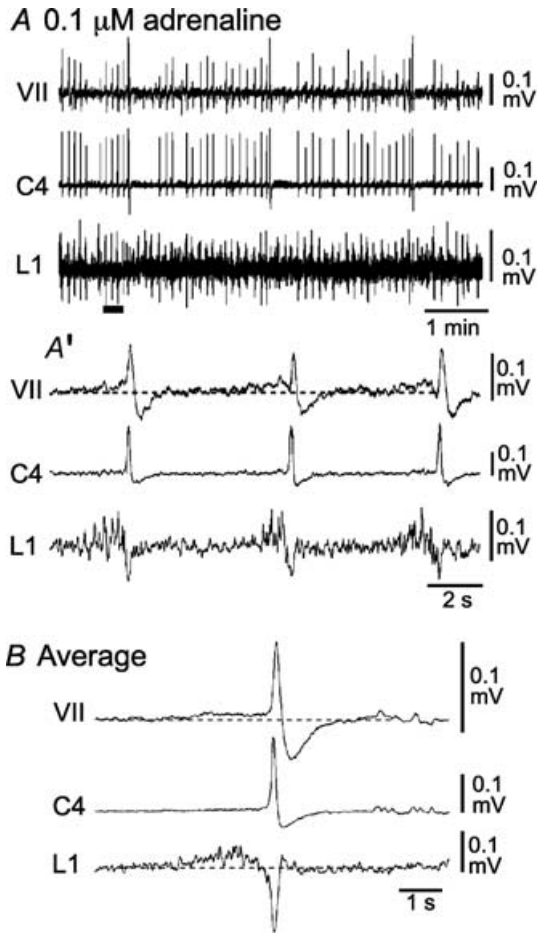

Figure 10. Respiration-related nerve activity in wild-type mice
A, facial nerve, C4 and L1 activities in a wild-type mouse in the presence of 0.1 μM adrenaline. *A*′, faster sweep representation of nerve activity at the black bar in *A*. *B*, averaged nerve activity triggered by C4 (10 cycles). Note the clear preinspiratory activity in the facial nerve and L1 recordings. VII, facial nerve activity; C4, C4 inspiratory activity; L1, first lumbar ventral root activity. More irregular activity (in the same preparation) in the absence of adrenaline is shown in Supplemental Fig. 2.

faster burst rate than that of the inspiratory neurons, and the activity was associated with that of the facial nerve. Activity of these neurons was not inhibited by DAMGO, and the main region of activity extended more rostrally than that of the inspiratory neurons. Therefore, this group was thought to correspond to the pFRG/Pre-I neuron group (Takeda *et al.* 2001; Mellen *et al.* 2003; Onimaru & Homma, 2003; Onimaru *et al.* 2006). Some of the putative Pre-I neurons in *Atp1a2*$^{-/-}$ mice received EPSPs during the inspiratory burst. This type of connection has not been clearly described in previous studies of newborn rats. It remains to be resolved whether such a connection is specific to *Atp1a2*$^{-/-}$ mice or is preserved in wild-type mice or rats.

Coupling between the two rhythm generators

The two neuron groups in *Atp1a2*$^{-/-}$ mice did not show organized activation like that in wild-type mice. However, excitatory and inhibitory synaptic connections could exist between them, and coupling of Pre-I bursts to Insp bursts occurred after repeated application of adrenaline or substance P. The pattern of respiratory activity after application of neurostimulants in *Atp1a2*$^{-/-}$ mice resembled those of fictive eupnoea (faster rhythm) and sigh bursts (slower rhythm with larger amplitude), as described in slice preparations (Lieske *et al.* 2000). The fictive eupnia-like inspiratory burst was preceded by facial and L1 activity, which reflects medullary Pre-I neuron activity in the rat (Janczewski *et al.* 2002; Onimaru *et al.* 2006). Such fictive eupnoea-like inspiratory activity occurred only in the presence of neurostimulants (Figs 8 and 9) in *Atp1a2*$^{-/-}$ mice. Similar activity was observed in wild-type and heterozygous mice in the presence of a low concentration of adrenaline. These results are consistent with the notion that interaction between the pFRG/Pre-I rhythm generator and the pre-BötC/Insp rhythm generator is important for the production of respiratory rhythm in the brainstem–spinal cord preparation in rats (Mellen *et al.* 2003).

Spatial and temporal summation of EPSPs in Insp neurons during the preinspiratory phase may be important for the triggering of Insp bursts (Onimaru *et al.* 1997; Fujii *et al.* 2006*b*). When the summation of EPSPs reaches the activation threshold of Insp neurons, Insp burst activity is maintained by excitatory coupling among Insp neurons (Onimaru *et al.* 1997; Feldman & Del Negro, 2006; Fujii *et al.* 2006*b*). Therefore, the defective sequential activation of Pre-I and Insp neurons in *Atp1a2*$^{-/-}$ mice may be due to an abnormality of triggering of burst induction after summation of EPSPs in Insp neurons during the preinspiratory phase.

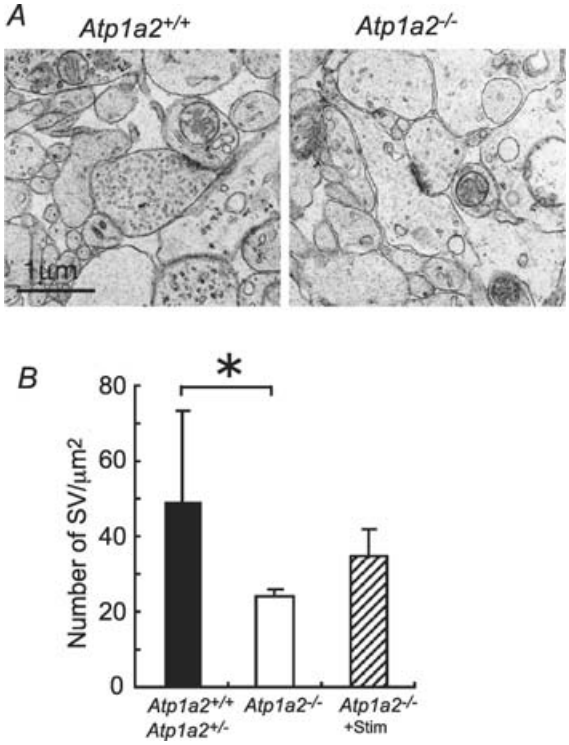

Figure 11. Electron micrographs of single synapses in the ventrolateral medulla of *Atp1a2*$^{+/+}$ or *Atp1a2*$^{+/-}$ and *Atp1a2*$^{-/-}$ mice

A, representative examples of presynaptic terminals with normal gross structural *Atp1a2*$^{+/+}$ and *Atp1a2*$^{-/-}$ features. Note the presence of fewer synaptic vesicles in the presynaptic region in *Atp1a2*$^{-/-}$ mice. *B*, quantitative analysis of synaptic vesicles (SV). Number of vesicles per μm^2 of presynaptic region of embryonic day 18.0–18.5 *Atp1a2*$^{+/+}$ or *Atp1a2*$^{+/-}$ ($n = 4$) and *Atp1a2*$^{-/-}$ ($n = 4$) fetuses. *Atp1a2*$^{-/-}$ + stim ($n = 3$) received repeated stimulation with 100 nM substance P. Data are means ± S.E.M. *$P < 0.04$.

Neurophysiological basis of the absence of respiratory neuronal activity in the fetal brainstem–spinal cord preparation of *Atp1a2*$^{-/-}$ mice

Results from previous studies (Moseley *et al.* 2003; Ikeda *et al.* 2004) do not fully explain why *Atp1a2*$^{-/-}$ mice show dysfunction of respiratory activity. The present findings, in addition to those from previous studies, clarify that the respiratory dysfunction of *Atp1a2*$^{-/-}$ mice is due to several closely linked abnormalities of respiratory neurons. One may involve an increased intracellular chloride concentration ($[Cl^-]_i$) caused by the functional uncoupling of the Na^+,K^+-ATPase $\alpha 2$ subunit and the neuron-specific K^+–Cl^- cotransporter KCC2. Increased $[Cl^-]_i$ plus excess extracellular GABA results in continuous membrane depolarization and causes failure of action potential generation due to inactivation of fast sodium channels (Ikeda *et al.* 2004). After the isolation of brainstem–spinal cords, the preparations show gradual recovery of neuronal reflex responses to electrical stimulation in the medulla because the extracellular GABA concentration is decreased, and the membrane potential

recovers (Ikeda *et al.* 2004). A second possible abnormality may involve poor connectivity between the two generators, as described in the present study. The decreased number of active synaptic vesicles near the active zone in the VLM neurons of *Atp1a2*$^{-/-}$ mice is consistent with this idea. Even after the recovery of neuronal activity, administration of a neurostimulant is required for the induction of respiration-like activity (Ikeda *et al.* 2004). The burst generation of these neurons disappeared in the absence of neurostimulant after repeated application (Fig. 8), indicating that there must be a lack of sufficient conditional inputs, such as excitatory inputs from chemoreceptors or other afferents, to burst generators in *Atp1a2*$^{-/-}$ mice.

The poor connectivity between the two generators and the lack of sufficient conditional inputs may result from weak neuronal activity during development. Accordingly, all motor activity, including respiratory movement, is inhibited in E18.5 *Atp1a2*$^{-/-}$ mice immediately after delivery by caesarean section (Ikeda *et al.* 2003, 2004).

Development of neuronal connections

During development, the pre-BötC/Insp rhythm generator is thought to emerge at late E16 to E17 (Pagliardini *et al.* 2003; Thoby-Brisson *et al.* 2005; Greer *et al.* 2006), and functional coupling with the pFRG/Pre-I rhythm generator becomes established at E19.5 in the rat (Onimaru & Homma, 2002, 2005). However, how these two generators develop to form a coupled oscillator and the functional significance of the interaction of these generators in newborn animals has not been addressed. *Atp1a2*$^{-/-}$ mice possess two functional generators, but their connectivity is not sufficient to drive spontaneous respiratory activity at birth (Ikeda *et al.* 2004). These observations indicate that each rhythm generator develops independently and that tight coupling of the two generators is critical for spontaneous rhythm generation after birth and hence for perinatal survival. Interestingly, connectivity could be partially restored by repeated stimulation in *Atp1a2*$^{-/-}$ mice, indicating that activity-dependent reinforcement of the connection, which normally occurs *in utero*, is critical for the formation of respiratory rhythm networks. The tight coupling of the generators may be the basis for the fine regulation of the respiratory rhythm in response to peripheral sensory and central inputs at later stages.

References

Arata A, Onimaru H & Homma I (1997). Low-concentration adrenaline modulates respiratory rhythm generating network in isolated brainstem-spinal cord preparation from newborn mouse. *Neurosci Res Suppl* **21**, s276.

Arata A, Onimaru H & Homma I (1998). Possible synaptic connections of expiratory neurons in the medulla of newborn rat in vitro. *Neuroreport* **9**, 743–746.

Ballanyi K, Onimaru H & Homma I (1999). Respiratory network function in the isolated brainstem-spinal cord of newborn rats. *Prog Neurobiol* **59**, 583–634.

Blanchi B & Sieweke MH (2005). Mutations of brainstem transcription factors and central respiratory disorders. *Trends Mol Med* **11**, 23–30.

Bocchiaro CM & Feldman JL (2004). Synaptic activity-independent persistent plasticity in endogenously active mammalian motoneurons. *Proc Natl Acad Sci U S A* **101**, 4292–4295.

Borday C, Wrobel L, Fortin G, Champagnat J, Thaeron-Antono C & Thoby-Brisson M (2004). Developmental gene control of brainstem function: views from the embryo. *Prog Biophys Mol Biol* **84**, 89–106.

Feldman JL & Del Negro CA (2006). Looking for inspiration: new perspectives on respiratory rhythm. *Nat Rev Neurosci* **7**, 232–242.

Feldman JL & Janczewski WA (2006). Point : Counterpoint: The parafacial respiratory group (pFRG)/pre-Bötzinger complex (preBötC) is the primary site of respiratory rhythm generation in the mammal. Counterpoint: the preBötC is the primary site of respiratory rhythm generation in the mammal. *J Appl Physiol* **100**, 2096–2097.

Fujii M, Umezawa K & Arata A (2006*a*). Adrenaline contributes to prenatal respiratory maturation in rat medulla-spinal cord preparation. *Brain Res* **1090**, 45–50.

Fujii M, Umezawa K & Arata A (2006*b*). Dopamine desynchronizes the pace-making neuronal activity of rat respiratory rhythm generation. *Eur J Neurosci* **23**, 1015–1027.

Greer JJ, Funk GD & Ballanyi K (2006). Preparing for the first breath: prenatal maturation of respiratory neural control. *J Physiol* **570**, 437–444.

Ikeda K, Onaka T, Yamakado M, Nakai J, Ishikawa TO, Taketo MM & Kawakami K (2003). Degeneration of the amygdala/piriform cortex and enhanced fear/anxiety behaviors in sodium pump α2 subunit (*Atp1a2)*-deficient mice. *J Neurosci* **23**, 4667–4676.

Ikeda K, Onimaru H, Yamada J, Inoue K, Ueno S, Onaka T, Toyoda H, Arata A, Ishikawa TO, Taketo MM, Fukuda A & Kawakami K (2004). Malfunction of respiratory-related neuronal activity in Na^+,K^+-ATPase α2 subunit-deficient mice is attributable to abnormal Cl^- homeostasis in brainstem neurons. *J Neurosci* **24**, 10693–10701.

Jacquin TD, Borday V, Schneider-Maunoury S, Topilko P, Ghilini G, Kato F, Charnay P & Champagnat J (1996). Reorganization of pontine rhythmogenic neuronal networks in *Krox-20* knockout mice. *Neuron* **17**, 747–758.

Janczewski WA & Feldman JL (2006). Distinct rhythm generators for inspiration and expiration in the juvenile rat. *J Physiol* **570**, 407–420.

Janczewski WA, Onimaru H, Homma I & Feldman JL (2002). Opioid-resistant respiratory pathway from the preinspiratory neurones to abdominal muscles: in vivo and in vitro study in the newborn rat. *J Physiol* **545**, 1017–1026.

Lieske SP, Thoby-Brisson M, Telgkamp P & Ramirez JM (2000). Reconfiguration of the neural network controlling multiple breathing patterns: eupnea, sighs and gasps. *Nat Neurosci* **3**, 600–607.

Lingrel J, Moseley A, Dostanic I, Cougnon M, He S, James P, Woo A, O'Connor K & Neumann J (2003). Functional roles of the α isoforms of the Na,K-ATPase. *Ann N Y Acad Sci* **986**, 354–359.

Mellen NM, Janczewski WA, Bocchiaro CM & Feldman JL (2003). Opioid-induced quantal slowing reveals dual networks for respiratory rhythm generation. *Neuron* **37**, 821–826.

Moseley AE, Lieske SP, Wetzel RK, James PF, He S, Shelly DA, Paul RJ, Boivin GP, Witte DP, Ramirez JM, Sweadner KJ & Lingrel JB (2003). The Na,K-ATPase α2 isoform is expressed in neurons, and its absence disrupts neuronal activity in newborn mice. *J Biol Chem* **278**, 5317–5324.

Onimaru H, Arata A, Arata S, Shirasawa S & Cleary ML (2004). In vitro visualization of respiratory neuron activity in the newborn mouse ventral medulla. *Brain Res Dev Brain Res* **153**, 275–279.

Onimaru H, Arata A & Homma I (1997). Neuronal mechanisms of respiratory rhythm generation: an approach using in vitro preparation. *Jpn J Physiol* **47**, 385–403.

Onimaru H & Homma I (1992). Whole cell recordings from respiratory neurons in the medulla of brainstem-spinal cord preparations isolated from newborn rats. *Pflugers Arch* **420**, 399–406.

Onimaru H & Homma I (2002). Development of the rat respiratory neuron network during the late fetal period. *Neurosci Res* **42**, 209–218.

Onimaru H & Homma I (2003). A novel functional neuron group for respiratory rhythm generation in the ventral medulla. *J Neurosci* **23**, 1478–1486.

Onimaru H & Homma I (2005). Developmental changes in the spatio-temporal pattern of respiratory neuron activity in the medulla of late fetal rat. *Neuroscience* **131**, 969–977.

Onimaru H & Homma I (2006). Point : Counterpoint: The parafacial respiratory group (pFRG)/pre-Bötzinger complex (preBötC) is the primary site of respiratory rhythm generation in the mammal. Point: the pFRG is the primary site of respiratory rhythm generation in the mammal. *J Appl Physiol* **100**, 2094–2095.

Onimaru H, Kumagawa Y & Homma I (2006). Respiration-related rhythmic activity in the rostral medulla of newborn rats. *J Neurophysiol* **96**, 55–61.

Pagliardini S, Ren J & Greer JJ (2003). Ontogeny of the pre-Botzinger complex in perinatal rats. *J Neurosci* **23**, 9575–9584.

Ptak K & Hilaire G (1999). Central respiratory effects of substance P in neonatal mice: an in vitro study. *Neurosci Lett* **266**, 189–192.

Rekling JC & Feldman JL (1998). PreBötzinger complex and pacemaker neurons: hypothesized site and kernel for respiratory rhythm generation. *Annu Rev Physiol* **60**, 385–405.

Smith JC, Ellenberger HH, Ballanyi K, Richter DW & Feldman JL (1991). Pre-Bötzinger complex: a brainstem region that may generate respiratory rhythm in mammals. *Science* **254**, 726–729.

Suzue T (1984). Respiratory rhythm generation in the in vitro brain stem-spinal cord preparation of the neonatal rat. *J Physiol* **354**, 173–183.

Sweadner KJ (1989). Isozymes of the Na^+/K^+-ATPase. *Biochim Biophys Acta* **988**, 185–220.

Takeda S, Eriksson LI, Yamamoto Y, Joensen H, Onimaru H & Lindahl SG (2001). Opioid action on respiratory neuron activity of the isolated respiratory network in newborn rats. *Anesthesiology* **95**, 740–749.

Thoby-Brisson M, Trinh JB, Champagnat J & Fortin G (2005). Emergence of the pre-Botzinger respiratory rhythm generator in the mouse embryo. *J Neurosci* **25**, 4307–4318.

Viemari JC & Ramirez JM (2006). Norepinephrine differentially modulates different types of respiratory pacemaker and nonpacemaker neurons. *J Neurophysiol* **95**, 2070–2082.

Acknowledgements

This study was supported by Grants-in-Aid for Scientific Research from the Japanese Ministry of Education, Culture, Sports, Science and Technology (MEXT) and by a High-tech Research Center Project for Private Universities matching fund subsidy from MEXT, 2003-07.

Supplemental material

Online supplemental material for this paper can be accessed at:
http://jp.physoc.org/cgi/content/full/jphysiol.2007.136572/DC1
and
http://www.blackwell-synergy.com/doi/suppl/10.1113/jphysiol.2007.136572